

# Kinetics and Mechanism of the CO shift on Cu/ZnO

## II. Kinetics of the Decomposition of Formic Acid

T. VAN HERWIJNEN,<sup>1</sup> R. T. GUCZALSKI,<sup>2</sup> AND W. A. DE JONG<sup>3</sup>

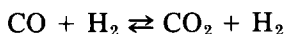
*Laboratory of Chemical Technology, Delft University of Technology, 136 Julianalaan, Delft, The Netherlands*

Received May 5, 1978; revised July 13, 1979

The decomposition of formic acid over the Cu/ZnO catalyst used in earlier work on CO shift kinetics has been examined. The reaction proceeds through a formate-type surface intermediate, the decomposition of which is rate determining. Surface coverage is rather high. The rate of formic acid decomposition is similar to that of the forward shift reaction and shows about the same temperature dependence. Both reactions as well as the reverse CO shift proceed via a surface intermediate of the same overall atomic composition. The high selectivity for formic acid dehydrogenation is in line with the value of about 50 found for the ratio between the rates of forward and reverse shift reactions. It is concluded that the kinetics of the CO shift conversion over Cu/ZnO catalyst are consistent with a mechanism in which the decomposition of a stable formate-type surface intermediate is rate determining.

### INTRODUCTION

Low-temperature shift Cu/ZnO catalysts are applied commercially on a very large scale to obtain high CO conversion at low-temperature levels, the conversion of carbon monoxide by conventional high-temperature iron oxide-based catalysts being limited by thermodynamic equilibrium. In a previous paper, the kinetics of the forward and reverse shift reactions over a commercial Cu/ZnO catalyst have been published (1). The equations for the initial rates of the reaction



in the forward and reverse directions show that the experimental results can be explained on the basis of rate control by a decomposition of coadsorbed complexes,  $\text{CO} \cdot \text{H}_2\text{O}$  and  $\text{CO}_2 \cdot \text{H}_2$ , respectively. The stoichiometry of these complexes corre-

sponds to formic acid and may be indicative of formate or formic acid-derived intermediates. Infrared spectroscopic studies of the water-gas shift reaction on oxide catalysts have revealed the presence of formate ions (2, 3) under typical reaction conditions. Armstrong and Hilditch (4) have postulated that the formation of a formic acid intermediate also applies to catalysis of the water-gas shift reaction by Cu/ZnO.

The present paper reports a study on the kinetics of formic acid decomposition on a commercial Cu/ZnO catalyst. Conclusions are drawn about the mechanism of catalysis of the CO shift reaction on Cu/ZnO by comparing the observed kinetics with the results obtained on the forward and reverse CO shift reaction.

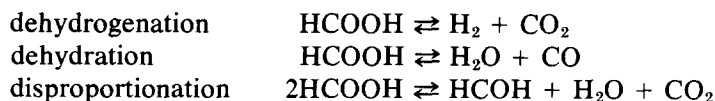
The gas-phase decomposition of formic acid has been studied extensively (5-8) and, in general, it has been found that the reaction proceeds via a formate complex. Among the many published investigations on this decomposition over metals and metal oxides are numerous kinetic studies. As early as 1911, Sabatier and Maihle (9) published data on the reaction over several

<sup>1</sup> Present address: Shell Coal International Ltd., London, U.K.

<sup>2</sup> Present address: Zakłady Chemiczne, Oświęcim, Poland.

<sup>3</sup> To whom correspondence should be addressed.

catalysts, including copper and zinc oxide. Three different reactions were formulated:



Copper and zinc oxide appeared to have high selectivities for dehydrogenation. Many subsequent papers deal with this topic, mainly in the context of theoretical studies on heterogeneous catalytic reactions. In the case of copper metal, it was reported that high coverages of stable surface formate were obtained (8). This extensive study by Sachtler and Fahrenfort (8) shows that a close relation exists between the activity for formic acid decomposition and the heat of formation of the corresponding formates, a relationship known as the volcano-shaped curve.

Kinetic studies have been published on the catalytic action of copper and of zinc oxide; publications on the mixed catalyst are not available. Measurements have shown that copper metal is an active catalyst for the dehydrogenation of formic acid with a selectivity of 99%. Kinetics have

generally been described as zero order for formic acid partial pressures between 10 and 30 mm Hg at 50–300°C. Table 1 summarizes the published results which have been plotted in Fig. 1. Temperature  $T_s$  in Fig. 1 indicates the isokinetic temperature, i.e., the temperature at which all catalysts have the same reaction rate within the accuracy of regression (10). These data are another illustration of the so-called compensation effect where changes in activation energy are compensated by variations in the frequency factor. This phenomenon may have some fundamental physicochemical cause but it may also be the result of modeling procedures, experimental accuracy, or selection of the experimental conditions. The description of the formic acid decomposition as a zero-order reaction adopted for the calculation of  $T_s$  is certainly incorrect (see Fig. 5).

TABLE 1  
Literature Data on the Kinetics of the Decomposition of Formic Acid over Copper<sup>a</sup>

Author	Catalyst	$p_{\text{HCOOH}}$ (mm Hg)	$T$ (°K)	$\log A$ (s <sup>-1</sup> )	$E$ (kcal/mole)	$T_s^b$ (°K)
1. Rienäcker (13)	Powder	30	393–413	9.9	22.3	492
2. Rienäcker (14)	Powder	25	373–433	8.0	15.6	426
	heated ½ h, 200°C					
3. Rienäcker (14)	Powder	25	373–433	6.1	12.6	451
	heated ½ h, 300°C					
4. Rienäcker (14)	Powder	25	373–433	6.8	14.6	469
	heated ½ h, 600°C					
5. Rienäcker (14)	Powder	25	373–433	9.2	19.3	458
	heated ½ h, 850°C					
6. Tamaru (7)	Reduced CuO	30	438–472	12.9	27.0	457
7. Schwab (15)	Copper sheet		520–600	10.0	24.4	533
8. Schwab (16)	Powder	30	319–354	14.1	29.3	454
9. Quinn (17)	Powder	10–25	353–473	10.6	24.2	498
10. Inglis (18)	Film	30	373–573	11.4	26.8	513

<sup>a</sup> All powders were electrolytically prepared.

<sup>b</sup> Calculated for  $r = 1$  molecule/(site · s).

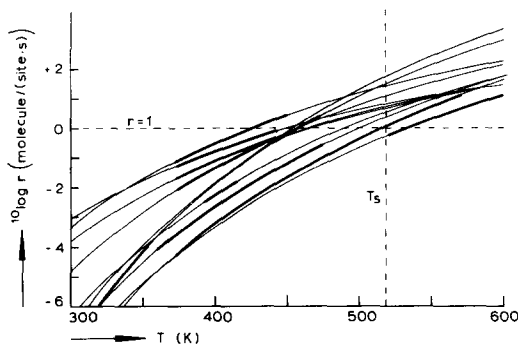


FIG. 1. Rate of reaction calculated from the published results shown in Table 1. The thick part of each line corresponds to the interval explored in the study.

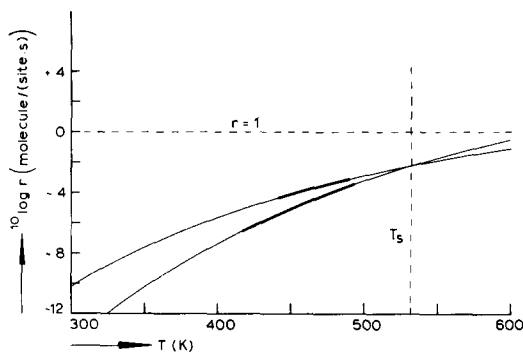


FIG. 2. Rate of reaction calculated from data reported in Table 2. The thick part of each line corresponds to the interval explored in the study.

From the combined published reaction rates, an average rate is estimated for the dehydrogenation of formic acid over copper catalysts:

$$\log(r) = 10.0 - 22,000/2.303RT \pm 1.5, \quad (1)$$

with  $r$  expressed in molecules/(site · s),  $T$  in K and  $R$  in cal/mole · K). Quantitative studies of the catalytic effect of zinc oxide report a high selectivity toward dehydrogenation (85–100%). Measurements at 10–20 mm Hg formic acid partial pressure and 150–200°C have been described by zero-order kinetics. Table 2 summarizes the published rate constants and Fig. 2 shows the corresponding rate versus temperature curve. From this rather limited information, an average rate equation is estimated for the dehydrogenation of formic acid over

zinc oxide catalysts:

$$\log(r) = 10.0 - 30,000/2.303RT, \quad (2)$$

where  $r$  is expressed in molecules/(site · s).

Activity wise, a mixed copper/zinc oxide catalyst can be regarded as a copper catalyst, assuming interactions to be absent, since for the temperature range of 100–250°C the rate over copper is 2000 to 15,000 times faster than the rate over zinc oxide. The effect of interactions, if any, cannot be predicted. It has been shown (11) that under the prevailing conditions zinc can dissolve in copper to form an alpha brass. This affects the electronic structure of the metal phase as well as the lattice constants, both of which may have an effect on the rate of reaction. A third factor of importance can be a change in electron concentration in the copper phase due to electrical

TABLE 2

Literature Data on the Kinetics of the Decomposition of Formic Acid over Zinc Oxide

Author	Catalyst	$P_{\text{HCOOH}}$ (mm Hg)	$T$ (°K)	$\log A$ (s <sup>-1</sup> )	$E$ (kcal/mole)	$T_r^a$ (K)
1. Schwab (19)	Zn(OH) <sub>2</sub> calcined		420		30	
2. Szabó (20)	ZnO calcined at 1200°C				23	
3. Hirota (21)	ZnCO <sub>3</sub> calcined at 470°C	20	443–483	8.03	25 ± 2	454
4. Tamaru (22)	ZnCO <sub>3</sub> calcined at 420°C	10–20	418–493	13.0	37.1	477

<sup>a</sup> Calculated for  $r = 0.0001$  molecule/(site · s).

contact between metal and semiconductor.

### EXPERIMENTAL

Kinetic measurements have been conducted with formic acid in nitrogen in a continuous-flow microreactor at 1-bar total pressure and temperatures between 130 and 160°C (Fig. 3). Gases were dried with molecular sieves and cleaned with BTS catalyst (BASF R3-1), and formic acid was added by passing nitrogen through a saturator filled with formic acid immersed in a thermostatic bath. The mole fraction of formic acid was varied by changing the temperature of the bath; this system was calibrated taking gas-phase dimerization of formic acid into account. The reactants flowed through heated tubes to a microreactor of 55-mm length and 7-mm i.d. made from chromium steel. The catalyst, Girdler G66B, of sieve fraction 0.35 to 0.42 mm, was diluted with quartz of the same size to fill the reactor completely. The reactor was immersed in a thermostatic bath of molten salt, the temperature of which was kept constant within 0.15°C.

Product gases were analyzed over a Porapak Q column after removing water and unconverted formic acid by freezing with a CO<sub>2</sub>-alcohol mixture. The conversion was calculated from the CO<sub>2</sub> content using nitrogen as an internal standard. Low concentrations of CO were determined with Dräger CO-selective indicator tubes, type 5/c, placed in the product line; the progress of the colored zone as a function of time was calibrated to serve as a measure of the CO content.

The catalyst was heated to 140°C in a nitrogen flow and reduced at that temperature for 16 h with 0.5%, 4h with 1.0%, and at least 2 h with 2% hydrogen in nitrogen. The reduced catalyst was stabilized for 3 days at 140°C with a mixture of HCOOH and nitrogen, molar ratio 1:12; this pre-

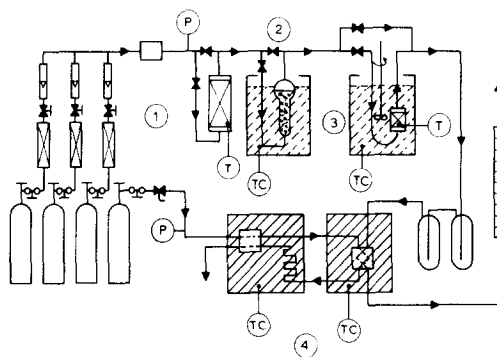


FIG. 3. Flow diagram of apparatus for kinetic experiments.

treatment obviated a correction for deactivation during the kinetic measurements. After completion of the experiments, the catalyst appeared to have a BET surface area of 3.6 m<sup>2</sup>/g.

### RESULTS

The kinetics of the decomposition of formic acid were determined using the initial rate approach. For each condition the rate was found from conversions observed at two to four space velocities. Separate exploratory measurements up to 16% conversion did not reveal deviations from the linear relationship between conversion and space velocity shown in Fig. 4. The observed CO concentration in the product gas corresponded to 98.5–99.5% selectivity for the dehydrogenation of formic acid.

Reaction rates were calculated from a least-squares fit to the data. The results in Fig. 5 show that the rate of decomposition approaches a limit value for each temperature; the kinetics change from first order at partial pressures of about 0.01 bar to zero order for partial pressures above 0.2 bar.

The observed dehydrogenation rates have been modeled with a Langmuir-type rate equation which in the most general form considered here reads:

$$r = \frac{k_{\infty} \exp(-E/RT) \cdot p_{\text{HCOOH}}}{(1 + K_0 \exp(-\Delta H/RT) \cdot p_{\text{HCOOH}})^m} \text{ moles}/(\text{g} \cdot \text{s}). \quad (3)$$

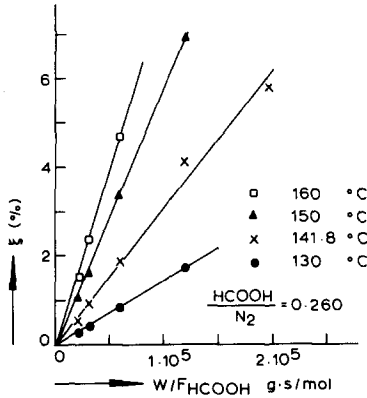


Fig. 4. Dependence of the conversion on the reciprocal space velocity.

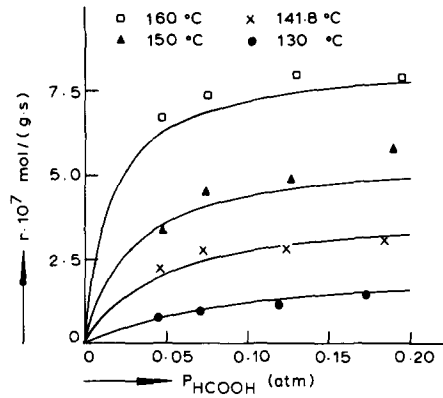


Fig. 5. Rate of formic acid dehydrogenation on Cu/ZnO.

As in the previous paper (1), nonlinear regression was applied to a set of rate equations. In this case four equations were studied assuming the adsorption constant for formic acid to be either constant or temperature dependent and assuming the exponent  $m$  to be one or variable. In the least-squares regression the square of the deviation between the observed rate and the calculated rate was weighted against the variance in the observed rate,  $S_{r,j}^2$ , as calculated from the conversion/space velocity data for a straight line through the origin. Thus, the objective of the nonlinear regression became:

$$\text{minimize } Q = \sum_j \frac{(r_{c,j} - r_{o,j})^2}{S_{r,j}^2}. \quad (4)$$

The four resulting model variances (30.9, 28.8, 25.4, and 24.9) are not significantly different at the 75% confidence level when the  $F$  test is applied to these data. It must be noted that, strictly speaking, the  $F$  test cannot be applied to nonlinear models although it certainly is indicative (12). For the rate equation it means that the simplest model with a constant adsorption equilib-

rium constant and exponent  $m$  equal to one gives a sufficiently accurate description; more parameters do not significantly improve the fit from a statistical point of view. When, however, the apparent energy of activation is calculated for the model with a constant adsorption constant ("model 1"), and for the model with a temperature-dependent adsorption constant for formic acid ("model 2") using the definition

$$E_a = \frac{\partial \ln(r)}{\partial (-1/RT)}, \quad (5)$$

a significant difference appears between the two models (Fig. 6). When in model 2,  $E_a$  is allowed to vary with the reaction conditions, one finds a rather wide spread over the range of conditions explored,  $E_a$  varying around the constant value of 21 kcal/mole obtained for model 1. Although strictly speaking the inclusion of the temperature dependence is statistically not justified, it is felt that the relatively large differences in  $E_a$  should be preserved in the model. For that reason the model with the temperature-dependent  $K$  value is preferred:

$$r = \frac{5.44 \times 10^{13} \exp(-35,700/RT) \cdot p_{\text{HCOOH}}}{1 + 2.48 \times 10^{12} \exp(-21,000/RT) \cdot p_{\text{HCOOH}}} \text{ moles/(g} \cdot \text{s)}. \quad (6)$$

It should be stressed here that this equation is a mathematical representation of our

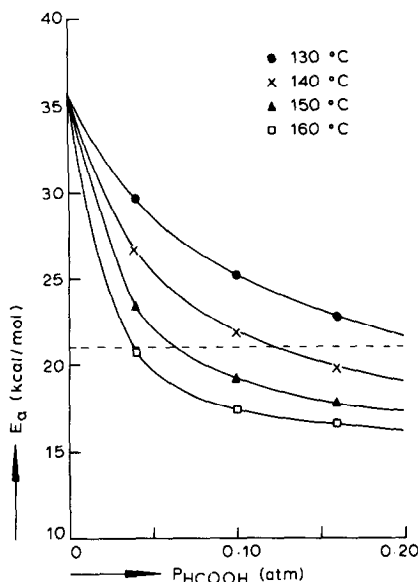


FIG. 6. Apparent energy of activation calculated with the equation with  $T$ -dependent adsorption constant; the dashed line corresponds to the constant- $K$  equation.

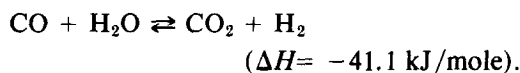
kinetic data rather than a physical model; the positive value for the  $\Delta H$  of adsorption of formic acid has no physical meaning. This is not serious because the kinetics are discussed below in terms of reaction rates rather than model parameter values.

To compare our result with the literature-derived rates over Cu and ZnO, the above rate equation was evaluated at 30 mm Hg formic acid partial pressure and the result expressed in molecules/(site  $\cdot$  s), assuming that half the BET surface area consists of copper surfaces with a site density of  $1.6 \times 10^{19}$  sites/m<sup>2</sup>. It appears from the results in Fig. 7 that the observed rate agrees fairly well with the rates reported for copper catalysts.

It is interesting to compare the energies of activation reported in the literature (Table 1) with the data of Fig. 6: within a range of 30°C at a partial pressure of 0.05 bar,  $E_a$  varies from 20 to 30 kcal/mole. This effect, which in fact goes back to the choice of the rate equation, may explain the spread in the literature data.

## DISCUSSION

The kinetics of the decomposition of formic acid over a commercial LTS Cu/ZnO catalyst were examined as part of a study on the kinetics and mechanism of the CO shift conversion over this catalyst:



Results on the kinetics of the forward and reverse CO conversion have been published in a previous paper (1). It was shown that the rate equations correspond to the decomposition of a mixed complex,  $\text{CO} \cdot \text{H}_2\text{O}$  or  $\text{CO}_2 \cdot \text{H}_2$ , as the rate-determining step.

The assumption that the intermediates for the forward and reverse reactions are identical with the surface intermediate of the formic acid decomposition is demonstrated in Fig. 8. This figure shows how formic acid decomposition rate and selectivity tie in with those of the CO conversion. In order to quantify this scheme, the rate data must be brought to the same standard. To that end, they were converted to the dimension molecules/(site  $\cdot$  s). Ex-

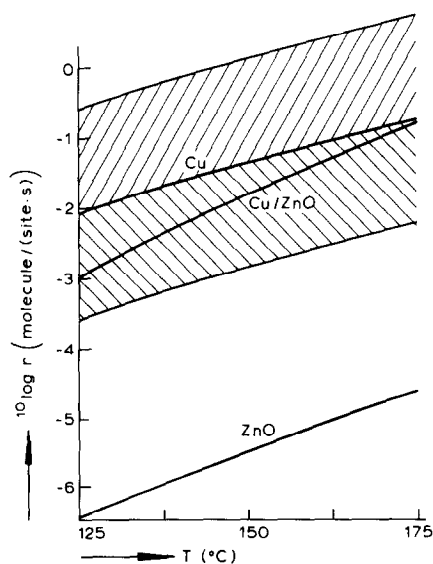


FIG. 7. Comparison of literature data on the dehydrogenation of formic acid over copper and zinc oxide with present results over copper/zinc oxide.

pressed as first-order decomposition rate equations, the kinetics are described by:

forward CO conversion,

$$r_f = 8.0 \times 10^5 \exp(-16,000/RT) \cdot \theta_{\text{CO}\cdot\text{H}_2\text{O}} \text{ molecules}/(\text{site} \cdot \text{s}), \quad (7)$$

reverse CO conversion,

$$r_r = 6.5 \times 10^7 \exp(-23,500/RT) \cdot \theta_{\text{CO}_2\cdot\text{H}_2} \text{ molecules}/(\text{site} \cdot \text{s}). \quad (8)$$

These equations were derived from the rate equations published in (1), assuming 50% of the BET surface area to consist of copper surfaces with a site density of  $1.6 \times 10^{19}$  sites/m<sup>2</sup>.

The rate equation for formic acid dehydrogenation (6) can be transformed into

$$r_d = 4.6 \times 10^5 \exp(-14,700/RT) \cdot \theta_{\text{HCOOH}} \text{ molecules}/(\text{site} \cdot \text{s}). \quad (9)$$

In Fig. 9 the calculated values of decomposition rate constants are shown as a function of temperature. The reaction rate constants of the dehydrogenation of formic acid and the decomposition of the CO · H<sub>2</sub>O intermediate in the CO conversion differ by a factor of 3–2 over the interval plotted; the temperature dependences are almost equal. Taking into account all approximations necessary for the evaluation of the rate constants in molecules/(site · s), it can be concluded that the rates of reaction are equal within experimental accuracy. Furthermore, the observed selectivity of 0.995–0.985 for dehydrogenation of formic acid corresponds very well with the factor 50 difference in

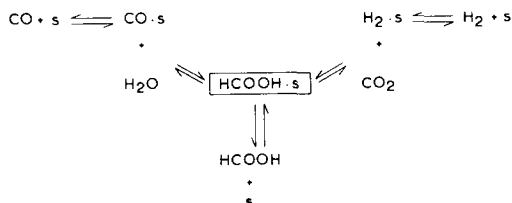


FIG. 8. Kinetic scheme for the forward and reverse CO conversion including the decomposition of formic acid.

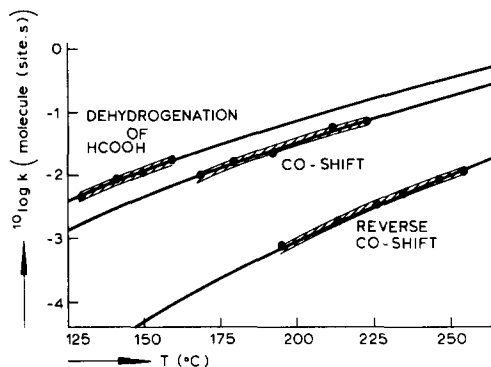


FIG. 9. Comparison of reaction rate constants. The heavier parts indicate the temperature range explored.

rates between the forward and reverse reaction. Since these rates have been determined as initial rates, i.e., far from the water–gas equilibrium, this clearly is a kinetic phenomenon.

It should be noted that the above conclusions on the rate constants for the surface reactions derive directly from the measured data and are not affected by the particular choice of the model equation. In order to show this, the occurrence of the “implicitly” measured quantities must be taken into account. In the previous paper (1) it was demonstrated that surface coverages are modeled together with the observed rate data, at least if the model equation allows one to do so. Coverage of a large part of the surface with the intermediate complex has been established in all three reactions. To demonstrate the consistency of the results, “observed” values for the rate constants were plotted in Fig. 9. These “observed” surface reaction rate constants were calculated from the observed rate of reaction and the surface coverage of the mixed complex under the prevailing conditions, as calculated from the parameters in the kinetic equations.

Attempts made to confirm the presence of formic acid or formate surface complexes on copper catalysts by ir spectroscopy experiments were unsuccessful because of the low transparency of the copper/zinc oxide system.

The kinetic studies produce one additional indication for the formic acid intermediate hypothesis. In Ref. (1), experiments at varying pressures were reported for the forward CO conversion. They show almost complete inhibition of the reaction at a conversion level that decreased with increasing pressure; this phenomenon has been ascribed to the formation of a surface complex of high stability. Explained more specifically as being caused by the formation of a formate complex, an equilibrium constant for its decomposition can be estimated. The result, about  $30 \text{ bar}^{-2}$ , agrees rather well with the value of  $35 \text{ bar}^{-2}$  calculated from Eq. (6) for the formic acid dehydrogenation.

As a result of these experimental studies it can be concluded that the kinetics of the CO conversion over a copper/zinc oxide catalyst can be described by a mechanism in which a stable formate intermediate is formed on the copper surface.

#### ACKNOWLEDGMENTS

We are indebted to Mr. C. W. A. Schram for his contribution to the theoretical part of this paper. We further gratefully acknowledge the grant one of the authors (R.T.G) received from the United Nations Technical Assistance Office, Geneva.

#### REFERENCES

1. van Herwijnen, T., and de Jong, W. A., *J. Catal.* **63**, 83 (1980).
2. Scholten, J. J. F., Mars, P., Menon, P. G., and van Hardeveld, R., in "Proceedings 3rd International Congress on Catalysis, Amsterdam, 1964," p. 881. Wiley, New York, 1965.
3. Tamaru, K., Uneo, A., Yamamoto, T., and Onishi, T., *Bull. Chem. Soc. Japan* **42**, 3040 (1969).
4. Armstrong, E. F., and Hilditch, T. P., *Proc. Roy. Soc. Ser. A* **97**, 265 (1920).
5. Mars, P., Scholten, J. J. F., and Zwietering, P., in "Advances in Catalysis and Related Subjects (D. D. Eley, H. Pines, and P. B. Weisz), Vol. 14, p. 35. Academic Press, New York, 1963.
6. Hirota, K., Kuwata, K., and Nakai, Y., *Bull. Chem. Soc. Japan* **31**, 861 (1958).
7. Tamaru, K., *Trans. Faraday Soc.* **55**, 1191 (1959).
8. Sachtler, W. M. H., and Fahrenfort, J., "Actes du Deuxième Congrès International de Catalyse," p. 831. Edition Technip, Paris, 1961.
9. Sabatier, P., and Maihle, A., *C. R. Acad. Sci.* **152**, 1212 (1911).
10. Cremer, E., in "Advances in Catalysis and Related Subjects" (W. G. Frankenburg, V. I. Komarewsky, and E. K. Rideal, Eds.), Vol. 7, p. 75. Academic Press, New York, 1955.
11. van Herwijnen, T., and de Jong, W. A., *J. Catal.* **34**, 209 (1974).
12. Draper, N. R., and Smith, H., "Applied Regression Analysis," Chap. 10. Wiley, New York, 1966.
13. Rienäcker, G., and Hildebrandt, H., *Z. Anorg. Allg. Chem.* **248**, 52 (1941).
14. Rienäcker, G., and Bremer, H., *Z. Anorg. Allg. Chem.* **272**, 126 (1953).
15. Schwab, G. M., and Schwab-Agallidis, E., *Ber. Deut. Chem. Ges.* **76**, 1228 (1943).
16. Schwab, G. M., and Watson, A. M., *Trans. Faraday Soc.* **60**, 1833 (1964).
17. Quinn, D. F., and Taylor, D., *J. Chem. Soc. A*, 5248 (1965).
18. Inglis, H. S., and Taylor, D., *J. Chem. Soc. A*, 2985 (1969).
19. Schwab, G. M., and Schwab-Agallidis, E., *J. Amer. Chem. Soc.* **71**, 1806 (1949).
20. Szabó, Z. G., Batta, I., and Solymosi, F., *Z. Phys. Chem. N.F.* **17**, 125 (1958).
21. Kondo, T., Ogawa, T., Kishi, K., and Hirota, K., *Z. Phys. Chem. N.F.* **67**, 284 (1969).
22. Noto, Y., Fukuda, K., Onishi, T., and Tamaru, K., *Trans. Faraday Soc.* **63**, 3081 (1967).